Condensation heat transfer and pressure drop correlations in plate heat exchangers for heat pump and organic Rankine cycle systems

Zhang, Ji; Elmegaard, Brian; Haglind, Fredrik

Published in:
Applied Thermal Engineering

Link to article, DOI:
10.1016/j.applthermaleng.2020.116231

Publication date:
2021

Document Version
Peer reviewed version

Condensation heat transfer and pressure drop correlations in plate heat exchangers for heat pump and organic Rankine cycle systems

Ji Zhang*, Brian Elmegaard, Fredrik Haglind

Department of Mechanical Engineering, Technical University of Denmark, Nils Koppels Allé, Building 403, 2800 Kongens Lyngby, Denmark

Abstract

An accurate prediction method of flow condensation heat transfer in plate heat exchangers is important for the design of condensers. The existing prediction methods are semi-empirical correlations, whose applicability highly rely on the range of original test data used for the correlation development. In this study, prediction methods of frictional pressure drop and heat transfer coefficient of flow condensation in a plate heat exchanger which were tailored for the applications in heat pump and organic Rankine cycle systems, were developed. We conducted a comprehensive experimental investigation, building a database including 283 data points for both pressure drop and heat transfer. We tested seven working fluids, classified by hydrofluorocarbons – R134a, R236fa and R245fa, hydrofluoroolefins – R1234ze(E) and R1233zd(E), and hydrocarbons – propane and isobutane, for a wide range of condensation temperatures varying from 30 °C to 90 °C. Two dimensionless numbers, the density ratio of liquid phase to vapour phase and the Bond number, were involved for developing the new prediction methods. The paper presents data for higher temperatures than those presented in previous works, and novel analysis and prediction methods. The new correlations achieve an improved prediction, enabling an 8.9 % and a 10.3 % mean absolute percentage deviation for heat transfer and pressure drop data, respectively.

Keywords: condensation, plate heat exchanger, high condensation temperature, correlation

Nomenclature

Symbols

b	corrugation amplitude, m
Bd	Bond number
D_h	hydraulic diameter, m
f	friction factor
G	mass flux of working fluid, kg/m^{2}s
h	heat transfer coefficient, W/m^2 K
k	thermal conductivity, W/m K
N	number of the plate
Nu	Nusselt Number
P	pressure, Pa
Pr	Prandtl number
Re	Reynolds number
T	temperature, °C
x	vapour quality

Greek Symbols

μ	dynamic viscosity, Pa s
ρ	mass density, kg/m^3
ρ^*	density ratio of liquid phase to vapour phase
Δ	difference
σ	surface tension, N/m

Subscripts

eq	equivalent
exp	experimental
fri	frictional
l	liquid
m	mean
out	outlet
pred	predicted
sat	saturation
sub	subcooled
sup	superheated
v	vapour
wf	working fluid

Abbreviations

HC	hydrocarbon
HFC	hydrofluorocarbon
HFO	hydrofluoroolefin
MAPD	mean absolute percentage deviation
ORC	organic Rankine cycle

* Corresponding author. Tel.: +45 45 25 13 87; fax: +45 45 25 19 61
E-mail address: jizhang@mek.dtu.dk (Ji Zhang)

β	chevron angle	PHE	plate heat exchanger
λ	wavelength of surface corrugation, m		
γ	dimensionless corrugation parameter		
φ	area enlargement factor		

1. Introduction

Plate heat exchangers (PHEs) consist of multiple chevron-corrugated plates; see Figs. 1 (a) and (b). The working fluid flows through a cross-corrugated channel formed by adjacent plates, in which the fluid path is further subdivided into numerous interconnected units by contact points of peaks and troughs of two adjacent plates; see Fig 1. (c). This complex flow morphology induces turbulence and enhances heat transfer [1]. The structure-determined advantages, e.g. thermal effectiveness, compactness and design flexibility, make the PHE increasingly used as condensers in a wide range of applications (e.g. organic Rankine cycle (ORC) [2] and heat pump systems [3]). Consequently, a reliable model for predicting the flow condensation heat transfer in PHEs is of crucial importance for the condenser design. An oversized or undersized design for the condenser will deteriorate the overall economic performance of the systems.

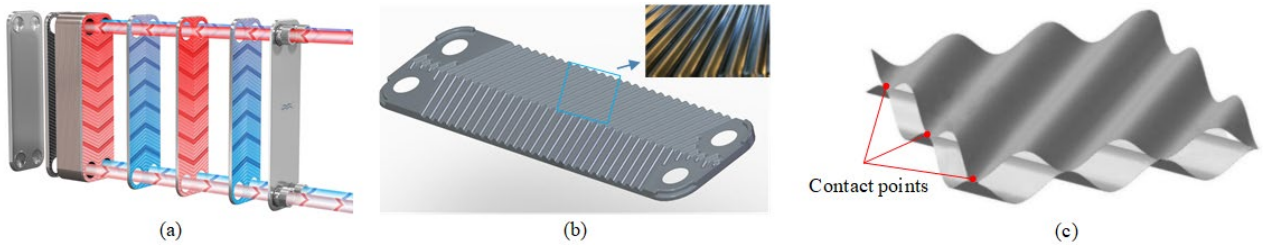

Figure 1. Illustration of (a) a PHE (by courtesy of Alfa Laval), (b) a chevron-corrugated plate, and (c) a cross-corrugated channel between two plates [4].

However, the complex flow morphology in the cross-corrugated channel makes it difficult to understand the internal two-phase flow. Vakili-Farahani et al. [5] recently carried out a review work on flow condensation in PHEs, and the authors stated that it is difficult to make theoretical predictions due to the limited studies in this field. Existing models used for predicting the condensation pressure drop and heat transfer coefficient in the cross-corrugated channels of PHEs are semi-empirical correlations developed using regression of experimental data. Tao and Ferreira [6] built a database including 2376 and 1590 data points for heat transfer and frictional pressure drop, respectively, to assess the predictive performances of the existing prediction methods. Although the correlations developed by Longo et al. [7] and Kuo et al. [8] showed the best accuracy among the eight heat transfer correlations selected in the paper, they are only able to predict 62.0 % and 58.5 % of the heat transfer data within ±30 % bandwidth, respectively. Up to 30 % deviation between the respective actual and predicted values is considered acceptable in industry [5]. It is even worse for the pressure drop correlation, i.e. the correlation developed by Amalfi et al. [9] only predicted 52.7 % of the pressure drop data within ±50 % bandwidth. This was even the best prediction result among those provided by the six selected pressure drop correlations. These results indicate that there is no reliable correlation that can be widely used for various applications.

Kim et al. [10] studied the two-phase flow in a channel of the PHE with a visualisation method. The authors observed that the two-phase flow in the millimetre-size PHE channel has similar thermo-physical characteristics as has been found in mini- and microchannels, i.e. bubbles can be elongated until fully approaching the diameter of the channel, which is different from turbulent mixing flow in conventional macroscale channels. Moreover, Amalfi et al. [9] suggested to introduce a parameter to characterise the transition between macro-to-microscale flow in PHEs, and separately develop the correlations for macro- and microscale heat transfer. The microscale heat transfer phenomenon identified in [9,10] suggests that the surface tension whose effects are usually negligible in macroscale channels, becomes important in PHE condensation [11]. The convection between the vapour and liquid phases can be affected by the surface tension, through a modification of liquid phase behaviour [12]. In our previous work [13], a widely used correlation (Yan et al. [14]) was modified by introducing a dimensionless number, the Bond number, which involves the surface tension, and thereby an improvement of the predictive performance of the new correlation for the experimental results was demonstrated. To the best of our knowledge, no other research work has incorporated the effects of surface tension when developing prediction methods of the thermal-hydraulic performance of condensation in PHEs.

High temperature condensation has numerous applications. One of the most typical applications is large-scale heat pumps connected to district heating systems. A survey for Europe indicates that 70 °C to 80 °C is the most common condensation temperature, and some systems operate at even higher temperatures [15]. In addition, this high temperature condensation is also applied in ORC systems used for combined heat and power generation (e.g. [16]). As previously mentioned, the applicable range of existing correlations highly relies on the original operating conditions of the experimental results used for deriving the correlations. Nevertheless, the condensation temperatures in almost all the studies were concentrated between 20 °C and 40 °C, and only a few tests were carried out with relatively high temperatures up to about 70 °C [6,13]. It is well known that the saturation temperature is an important factor in the condensation process, and the heat transfer can be enhanced by increasing the saturation temperature, meanwhile with an increased pressure drop [5]. Therefore, the applicability of existing condensation correlations for high temperature conditions needs to be evaluated.

The goal of this paper is to develop prediction methods of the thermal-hydraulic performance for the flow condensation in PHEs that can be widely applicable for the working conditions in condensers of heat pump and ORC systems. In order to achieve this goal, a series of experiments was carried out with condensation temperatures varying from 30 °C to 90 °C and with various mass flow rates. Specifically, the (40 to 90) °C and (30 to 50) °C condensation temperatures are commonly applied in the condenser of heat pump and ORC systems, respectively [2,17] and the high temperatures of (70 to 90) °C are also applicable for the condenser in ORC-based combined heat and power plants [16]. Seven working fluids commonly used in the two systems [17,18] were selected for the experimental tests; these consisted of three hydrofluorocarbons (HFCs), R245fa, R236fa and R134a, two hydrofluoroolefins (HFOs), R1233zd(E) and R1234ze(E), and two hydrocarbons (HCs), isobutane and propane. Subsequently, we carried out an experimental analysis to identify the most important parameters (among which the surface tension is considered) and used the test data to evaluate the existing correlations' predictive performances. Based on the analysis, the identified parameters were integrated with the existing correlations to develop the new prediction methods.

The paper includes the following novel contributions. First, the flow condensation characteristics under the high temperature condensation (70 °C to 90 °C) were systematically investigated, while relevant recent works targeted temperatures lower than 70 °C [6,13]. Second, the experimental results and thermo-physical properties of seven working fluids were compared, aiming at identifying the most influential parameters on thermal-hydraulic performance. Such comparison among different working fluids is lacking in the existing research works. Third, two dimensionless parameters, the density ratio of liquid phase to vapour phase and the Bond number, were used for developing the new prediction methods. In addition, based on our previous study [13] we improve the condensation process used for the acquisition of experimental data, i.e. excluding the liquid subcooling region from the whole condensation process and thus improving the accuracy of condensation data (see Section 2.1).

Section 2 presents the methods of the experimental campaign, data reduction and uncertainty analysis. Section 3 presents experimental results of PHE condensation, a comparison of thermal-hydraulic performance among the working fluids, an evaluation of predictive performance of existing correlations for the test data and a development of new prediction methods. Important findings and conclusions are presented in Section 4 and Section 5, respectively.

2. Methods

2.1 Experimental campaign

A PHE test facility at the Technical University of Denmark was used for the experiments. A brazed PHE having a 3.4 mm hydraulic diameter D_h and a 65^o chevron angle β is placed in the working fluid loop and used as the test section (condenser). Further details of the test facility and the PHE geometry can be found in [13].

Table 1 summarises the differences in working conditions between the present study and the previous work [13]. First, three new working fluids (R236fa, isobutane, propane) were added, especially the inclusion of a new type of working fluid, HC that has significantly different thermo-physical properties than those of HFCs and hydrofluoroolefin HFOs (e.g. HCs have much lower density of the liquid phase). Second, the range of condensation temperatures used for testing was extended, i.e. the lower temperature for all working fluids is 30 °C, while the upper temperature of four of the working fluids is 90 °C. Third, the working fluids were controlled as the saturated liquid with the vapour quality of 0.01 to 0.05 at the outlet of the condenser. In the

previous study [13], the condensation process in the condenser included also the liquid subcooling region, characterised by a subcooling of (0 to 5.3) K at the outlet of the condenser. Accordingly, the liquid subcooling region was excluded from the whole heat transfer process in the data reduction of previous work [13]. The liquid single-phase heat transfer coefficient and the frictional pressure drop in the subcooling region, and thus the heat transfer area of the subcooling region, were estimated using existing single-phase flow correlations, which may ultimately cause deviations in the results of condensation heat transfer from actual values. In general, the working conditions used in the present study will be beneficial for developing condensation correlations enabling an improved accuracy and a wider applicable range both in terms of working fluids and temperatures. Moreover, the vapour at the inlet of the condenser kept the superheating within 5 K. The mass flux of the working fluids ranged from 12 kg/m^{2}s to 92 kg/m^{2}s. The Refprop 10.0 [19] was used to calculate the thermo-physical properties of the working fluid.

Table 1. Comparison of working conditions between the present and previous experiments [13].

	Working fluids	Condensation temperature	Working fluid condition at outlet of condenser
Present study	R236fa R245fa R1233zd(E) Isobutane	30 °C, 40 °C, 50 °C 70 °C, 80 °C, 90 °C	Two-phase fluid with a vapour quality of 0.01 to 0.05
	R134a R1234ze(E) Propane	30 °C, 40 °C, 50 °C	
Previous study [13]	R134a R1234ze(E)	30 °C, 40 °C 50 °C, 60 °C	Liquid subcooled 0.0 K to 5.5 K
	R245fa R1233zd(E)	40 °C, 50 °C 60 °C, 70 °C	

2.2 Data analysis

The data reduction method for the condensation process studied in the present paper, i.e. condensation of the working fluids from slightly superheated vapour to the almost saturated liquid, has been presented in our previous work [13]. The heat transfer coefficient h_{wf}, frictional pressure drop Δp_{fri}, friction factor f of the working fluid for flow condensation in the PHE as well as the other relevant parameters were calculated. Following the method suggested by Kline and McClintock [20], the uncertainties of h_{wf} and ΔP_{fri} were calculated based on those of the directly measured parameters, whose values can be found in [13]. The uncertainties of h_{wf} and ΔP_{fri} range from 3.9 % to 13.4 % and from 4.1 % to 14.8 %, respectively.

3. Results

3.1 Experimental results

For validation purposes, we compared the heat transfer results obtained in the present study with those from another study that carried out experiments using similar working conditions. Longo [21] tested the complete condensation of R134a, i.e. a superheating of about 10 K at the condenser inlet and a subcooling of about 3 K at the condenser outlet, which is closest to the working conditions used in the present research among the studies found in literature. The condensation heat transfer coefficients of R134a obtained in the present study and the study reported by Longo [21] are compared in Figure 2 under the same saturation temperature T_{sat} of 40 °C and almost the same range of mass fluxes of working fluid G. Figure 2 shows that the data points from Longo [21] fall in the uncertainty range of heat transfer results obtained in the present study, indicating an agreement between the results of the two studies.

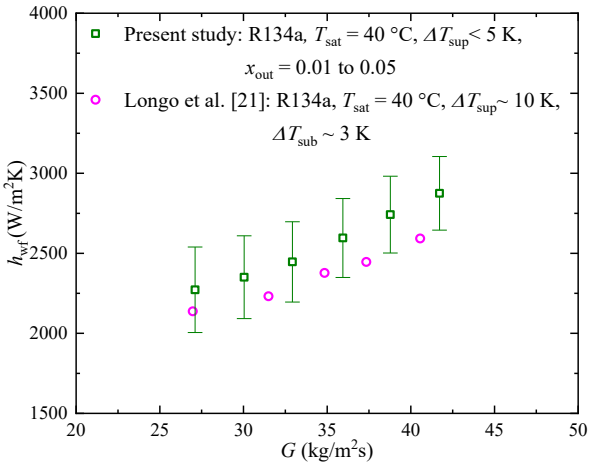

Figure 2. Comparison of h_{wf} of R134a obtained in the present paper and the study reported by Longo [21].

Figures 3 and 4 depict the test results of heat transfer and pressure drop of the seven working fluids with various working conditions. A wide range of heat transfer coefficients and length-specific frictional pressure drops (frictional pressure drop per unit length of the plate) were obtained in the study. Overall, the heat transfer coefficient and the length-specific frictional pressure drop vary from 1819 W/m^{2}K to 5242 W/m^{2}K and from 10.5 kPa/m to 108 kPa/m, respectively. The heat transfer coefficient and the frictional pressure drop of all working fluids increase with the mass flux and decrease with the saturation temperature, which is a typical characteristic of a shear-controlled condensation mainly realised by convective heat transfer at the interface of the liquid and vapour phases [5]. Moreover, this result is in line with the general findings concluded in the review work by Vakili-Farahani et al. [5]. In particular, both the higher mass flux and the lower saturation temperature enable a higher vapour velocity and thus more shear stress and turbulence at the liquid-vapour interface, resulting in an increased heat transfer coefficient and associated frictional pressure drop.

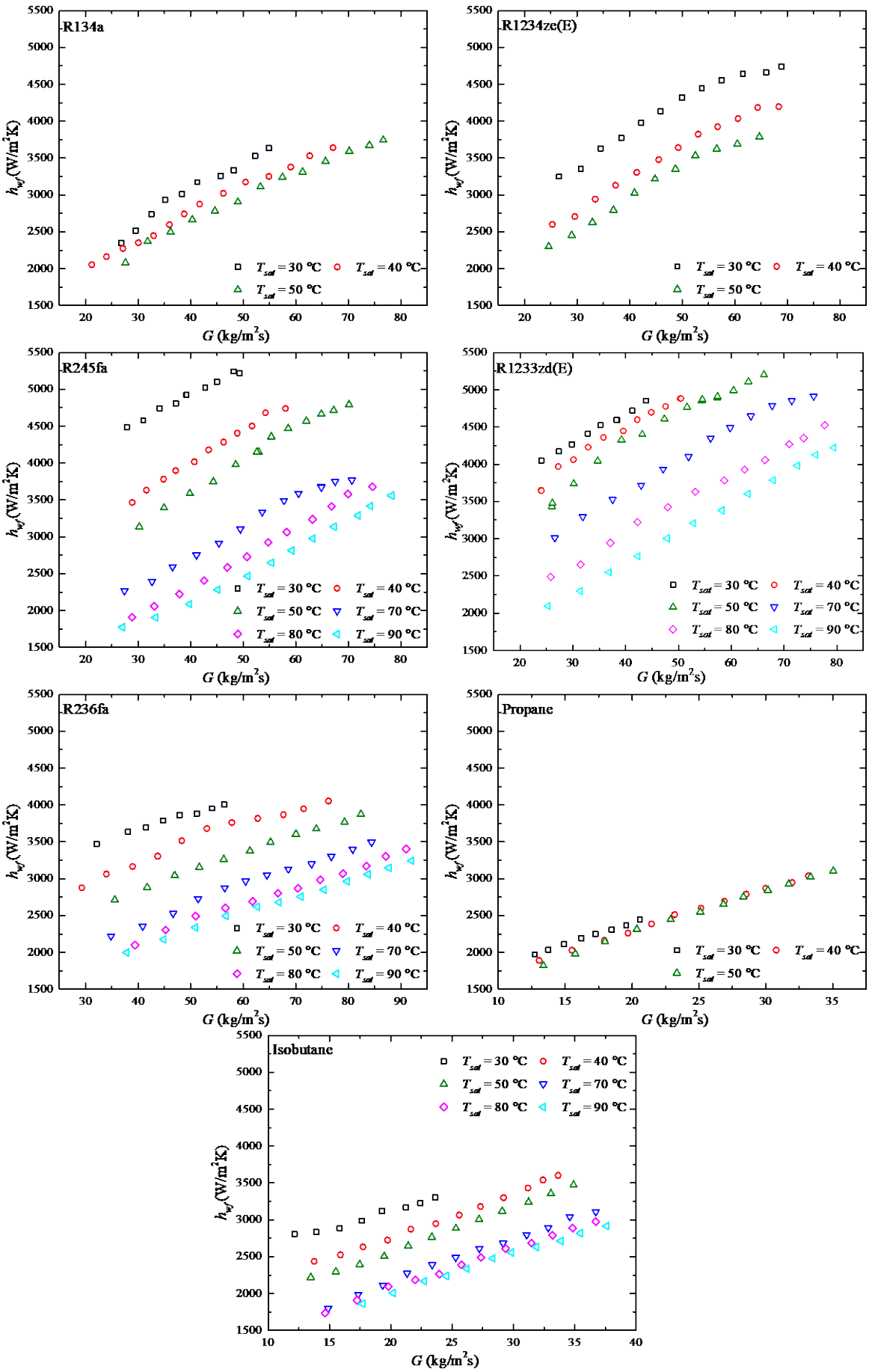

Figure 3. Heat transfer results of the seven working fluids.

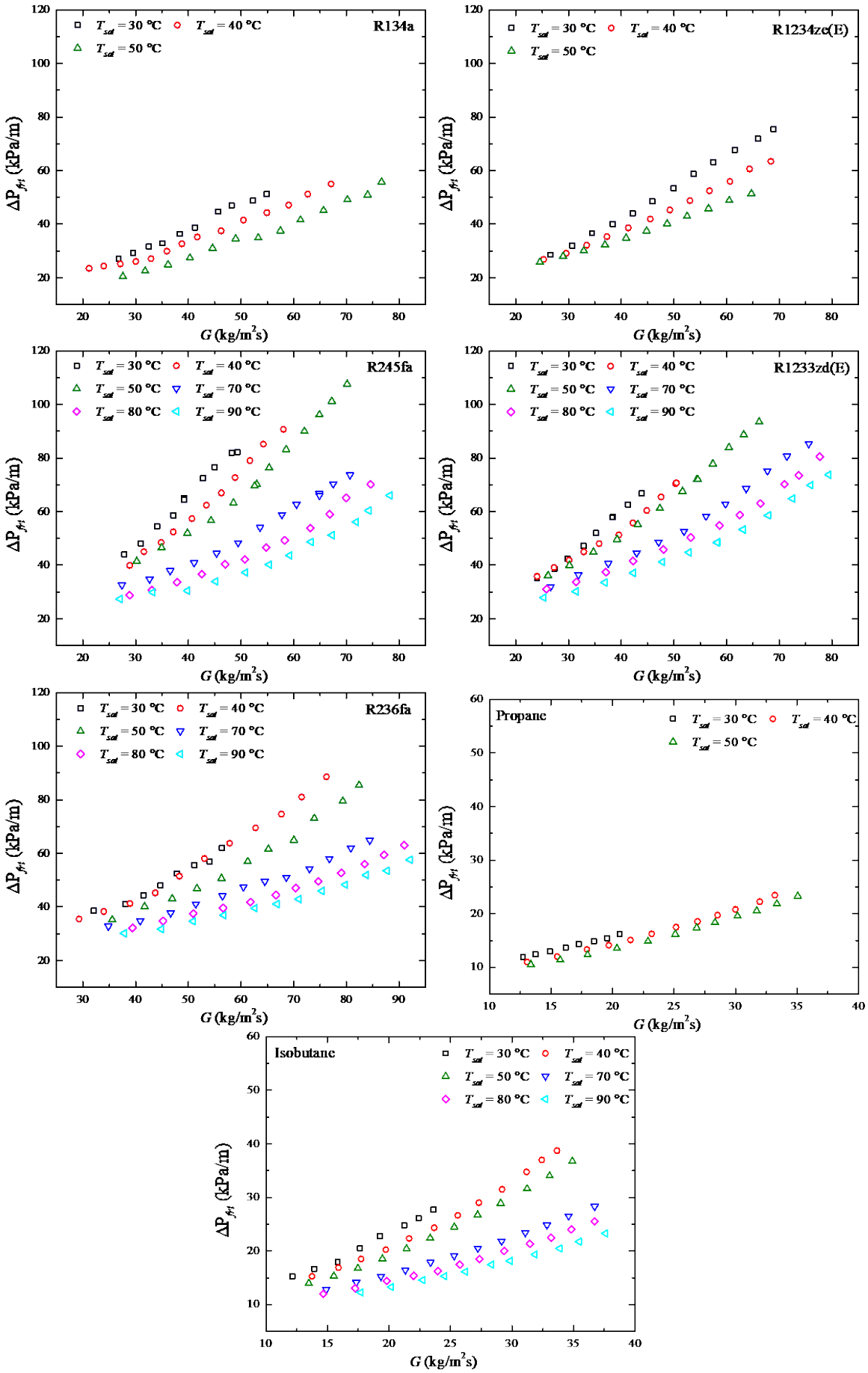

Figure 4. Pressure drop results of the seven working fluids.

3.2 Thermal-hydraulic performance comparison

In order to identify the parameters which are most influential on heat transfer and pressure drop, the experimental results of the seven working fluids are compared in this section. The comparison indicates that working fluids having the lower vapour density, ρ_v (higher vapour velocity), and higher surface tension, σ, generally have a better heat transfer performance. The vapour density and the surface tension of the seven working fluids are shown in Figure 5. Consequently, R1233zd(E), isobutane and R245fa have the highest h_{wf}, while R134a has the lowest h_{wf} among the seven working fluids used for T_{sat} = 30 °C to 50 °C experiments and R236fa has the lowest h_{wf} among the four working fluids used for T_{sat} = 70 °C to 90 °C experiments. For the frictional pressure drop, an influential parameter was identified, namely, the density ratio of liquid phase to vapour phase (see Figure 5), $\rho^* = \rho_l/\rho_v$, since the pressure drop among the different working fluids is correlated with their density ratios at a certain temperature. A larger liquid–vapour density difference means an increased shear stress of the vapour phase on the liquid phase, thus intensifying the convection at the interface and inducing a higher frictional pressure drop [22].

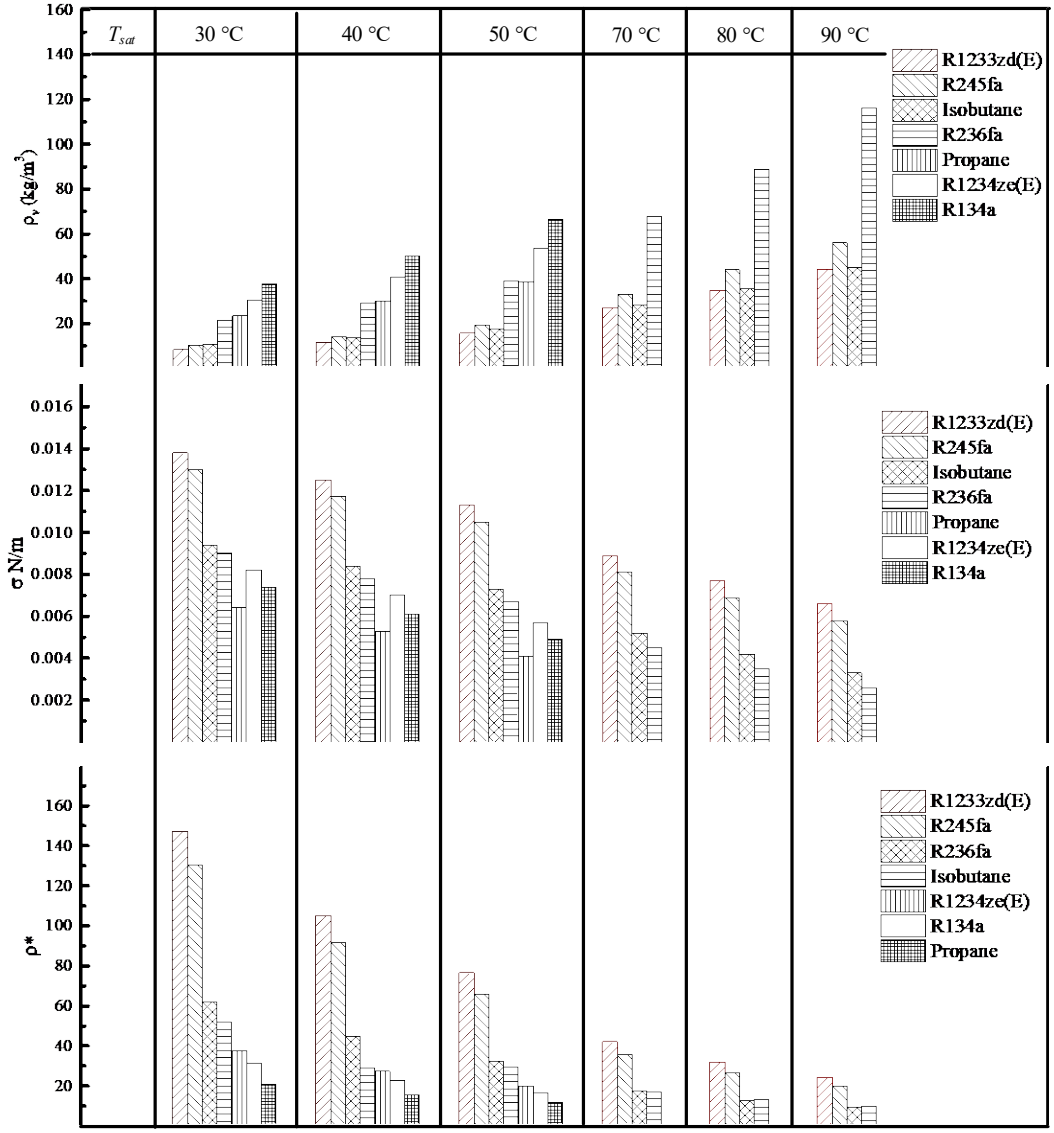

Figure 5. Thermo-physical property comparison of the working fluids at various temperatures.

For quantifying the thermal-hydraulic performance difference among the working fluids, an average h_{wf} and Δp_{fri} of each fluid was computed based on the same range of mass fluxes, and their differences are presented in Table 2. Isobutane was selected as the base fluid. No comparison was made for T_{sat} = 30 °C, because there is no common range of mass fluxes for propane and isobutene with other working fluids. From the table, the key findings with respect to the experimental test of the T_{sat} = 40 °C and 50 °C can be drawn as follows. First, R1233zd(E) has a 20 % and 16 % higher heat transfer coefficient than isobutane at T_{sat} = 40 °C and 50 °C, respectively. However, a 22 % increase in frictional pressure drop is also achieved by R1233zd(E) compared

with isobutane. Second, although propane has the weaker heat transfer performance compared to isobutane (11 % and 15 % lower heat transfer coefficient at T_{sat} = 40 °C and 50 °C, respectively), it enables a 37 % lower pressure drop. Third, the remaining working fluids, R245fa, R236fa, R134a and R1234ze(E), show less competition in the thermal-hydraulic performance, e.g. all of them have the lower h_{wf}, but higher Δp_{fri} than propane. In the experimental test of the T_{sat} = 70 °C to 90 °C, isobutane shows better performance than the other three working fluids, which is attributed to its highest h_{wf} and lowest Δp_{fri}.

Table 2. Differences of average h_{wf} and Δp_{fri} of working fluids when selecting isobutane as the base fluid.

	R1233zd	R245fa	R236fa	Propane	R134a	R1234ze(E)
40 °C	+20 %/+22 %	+5 %/+25 %	-14 %/+4 %	-15 %/-37 %	-31 %/-25 %	-19 %/-14 %
50 °C	+16 %/+22 %	-2 %/+26 %	-22 %/-4 %	-11 %/-37 %	-30 %/-35 %	-22 %/-15 %
	R1233zd	R245fa	R236fa			
70 °C	+12 %/ +45 %	-18 %/+37 %	-18 %/+24 %			
80 °C	-1 %/+46 %	-25 %/+32 %	-29 %/+26 %			
90 °C	-13 %/+44 %	-32 %/+30 %	-31 %/+30 %			

3.3 Evaluation of existing correlations

The heat transfer correlations derived by Longo et al. [7], Kuo et al. [8], Yan et al. [14] and Zhang et al. [13] were selected for the comparison. Tao and Ferreira [6] found that the correlations derived by Longo et al. [7], Kuo et al. [8] and Yan et al. [14] provide the best prediction for the database including 2376 heat transfer data points. These correlations are also the most commonly used in literature for condenser design. The correlation from Zhang et al. [13] was developed in our previous work [13]. Moreover, two pressure drop correlations derived by Amalfi et al. [9] and Zhang et al. [13] were considered in the present study. Amalfi et al. [9] built a database by collecting pressure drop data of evaporation in PHEs and derived a correlation using dimensional analysis-based multiple regression. The correlation derived by Amalfi et al. [9] was evaluated as the one having the best predictive performance by Tao and Ferreira [6].

The predicted values of the h_{wf} and Δp_{fri} using the selected existing correlations are shown in Figures 6 and 7, respectively. Furthermore, a parameter, namely the mean absolute percentage deviation (MAPD), was introduced to indicate the deviation between the predicted values using the selected correlation and the test results, calculated by

$$MAPD = \frac{1}{n}\sum_{i=1}^{n}\left|\frac{\mathrm{data_{i,pred}}-\mathrm{data_{i,exp}}}{\mathrm{data_{i,exp}}}\right| \times 100\%. \quad (1)$$

The correlation derived by Yan et al. [14] shows the best agreement with the heat transfer data, resulting in a MAPD of 15.2 %, but it provides a relatively weak prediction for the two HFOs, R1234ze(E) and R1233zd(E). The correlation derived by Longo et al. [7] provides a reasonable prediction for most of the data with a MAPD of 22.6 %. However, it underestimates almost all the results of R1233zd(E) and R1234ze(E) and the results of isobutane at low mass fluxes. The Kuo et al. [8] correlation underestimates most of the experimental results, with a MAPD of 33.6 %. The correlation from Amalfi et al. [9], though developed using the experimental data from evaporation two-phase flow, was able to provide a reasonable prediction for the Δp_{fri} with a 27.9 % MAPD, while slightly over-predicting the results of R245fa, R236fa and isobutane at high condensation temperatures, 70 °C to 90 °C. The correlation derived by Zhang et al. [13] provides good predictions for all working fluids with respect to both the h_{wf} and Δp_{fri}, but fails to predict the results of propane and isobutane. This may be attributed to the fact that the thermo-physical properties of these two HCs are quite different from those of the HFC and HFO working fluids involved in the database used to develop the correlation.

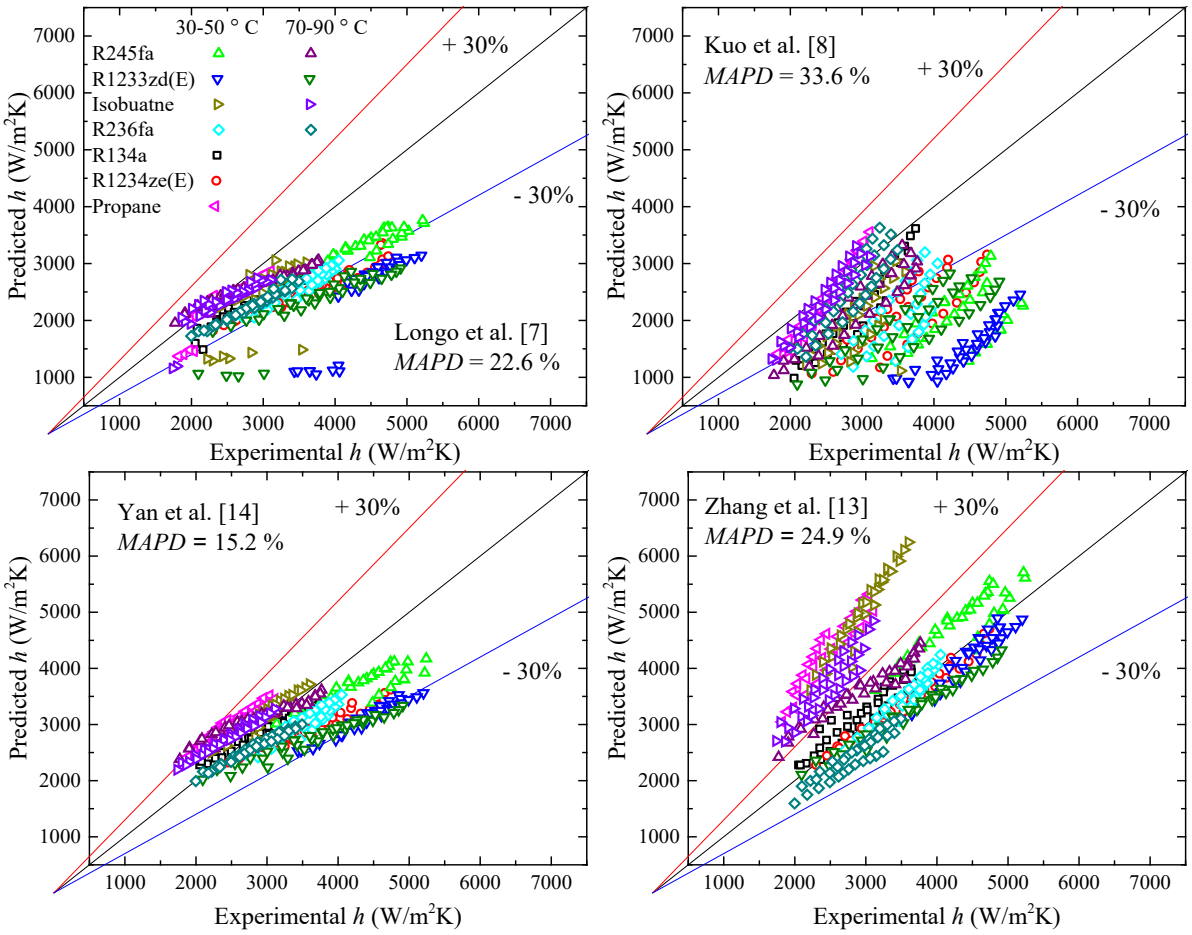

Figure 6. Predicted h_{wf} using the four selected correlations against the test results.

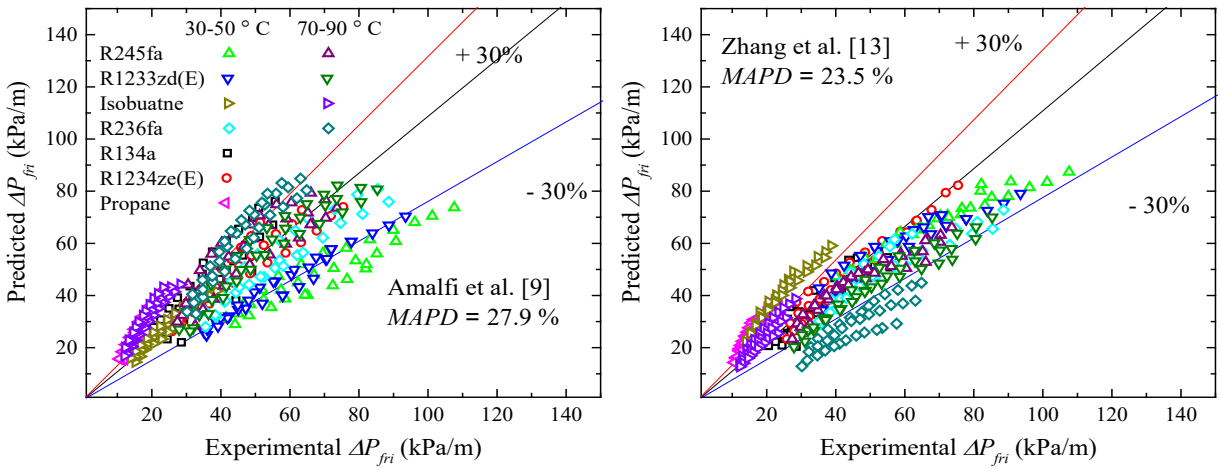

Figure 7. Predicted Δp_{fri} calculated by the two selected correlations against the test results.

3.4 New correlations

A new prediction method of heat transfer coefficient was developed in the present study, defined as

$$h_{wf} = 0.4703 Re_{eq}^{0.5221} Pr_l^{1/3} Bd^{0.1674} \rho^{*0.2126} (k_l/D_h), \quad (2)$$

where the hydraulic diameter D_h is defined as

$$D_h = 2b/\varphi, \quad (3)$$

where the b is the corrugation amplitude and the φ is the area enlargement factor caused by sinusoidal surface

waviness and is calculated by

$$\varphi = (1 + \sqrt{1+\gamma^2} + 4\sqrt{1+\gamma^2/2})/6, \quad (4)$$

where the γ is a dimensionless corrugation parameter, defined as

$$\gamma = \pi b/\lambda, \quad (5)$$

where the λ is the wavelength of surface corrugation

Eq. (2) was derived by modifying the correlation from Yan et al. [14]:

$$\mathrm{Nu} = 4.118\mathrm{Re_{eq}}^{0.4}\mathrm{Pr_l}^{1/3}, \quad (6)$$

since it enables a best prediction for the experimental results among all selected correlations. Specifically, two dimensionless numbers, the density ratio (ρ^*) and the Bond number (Bd), were added in the correlation with a multiple regression of test data. The density ratio represents the shear stress of the vapour phase acting on the liquid phase, while the Bond number represents the ratio of the gravitational force to the surface tension, accounting for the transition between macro-to-microscale two-phase flows. The Bond number is defined as

$$\mathrm{Bd} = g(\rho_\mathrm{l} - \rho_\mathrm{v})D_\mathrm{h}{}^2/\sigma. \quad (7)$$

The $\mathrm{Pr_l}$ is the Prandtl number of the liquid phase and the $\mathrm{Re_{eq}}$ is the equivalent Reynolds number, defined as

$$\mathrm{Re_{eq}} = G_\mathrm{eq}D_\mathrm{h}/\mu_\mathrm{l}, \quad (8)$$

where the μ_l is the liquid viscosity, and the equivalent mass flux G_eq is calculated by

$$G_\mathrm{eq} = G[1 - x_\mathrm{m} + x_\mathrm{m}(\rho_\mathrm{l}/\rho_\mathrm{v})^{0.5}], \quad (9)$$

where x_m is the mean vapour quality of the working fluid over the whole condensation process in which the inlet vapour quality is 1 in this study.

Likewise, a pressure drop correlation was derived by involving the density ratio and the Bond number:

$$f = 11557.62\mathrm{Re_{eq}}^{-1.0041}\mathrm{Bd}^{0.3002}\rho^{*-0.4268}. \quad (10)$$

The basic format $f = C\mathrm{Re_{eq}}^{n}$ is commonly used for developing PHE two-phase correlations in the literature (e.g. [23,24]). The predicted h_wf and f calculated by Eqs. (2) and (10), respectively, were compared with the test results, shown in Figure 8. The comparison suggests that the new correlations are able to predict 98 % of both the heat transfer and pressure drop data within the ±30 % bandwidth, having an 8.9 % and a 10.3 % MAPD, respectively. The ranges of the dimensionless numbers included in the correlations and the geometrical parameters of the PHE are presented in Table 3.

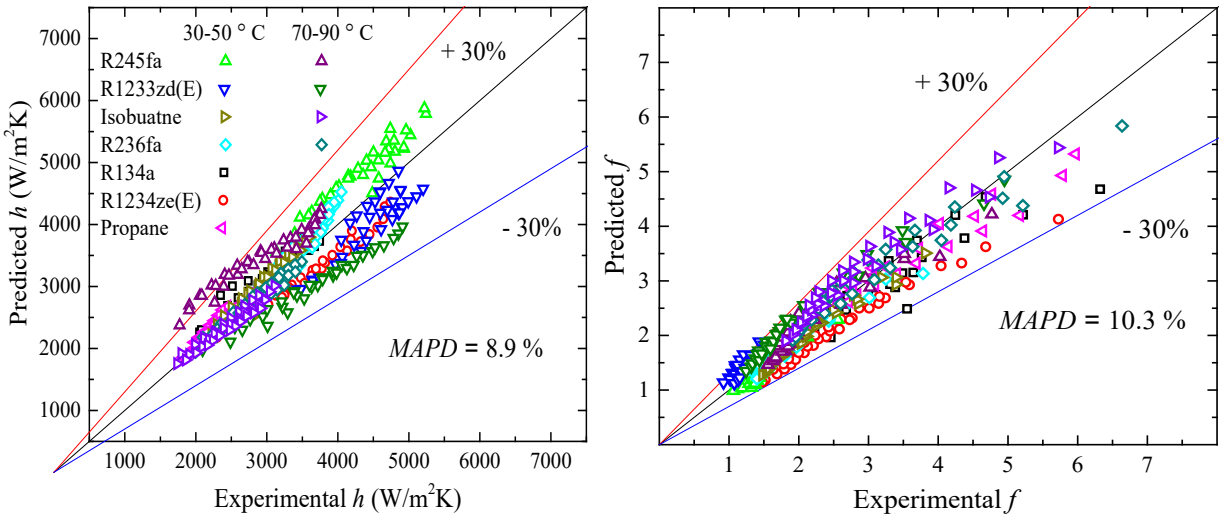

(a) (b)

Figure 8. Comparison between the predicted values using the proposed correlations (Eqs. (2) and (10)) and the test results for (a) h_{wf} and (b) f.

Table 3 Ranges of the dimensionless numbers included in the correlations and the geometrical parameters of the PHE.

Re_{eq}	Pr_l	Bd	ρ^*	D_h	β
1237 to 5240	2.8 to 7.5	6.3 to 42.4	9.2 to 149.0	3.4 mm	65 º

Table 4 Working conditions and PHE geometrical parameters used to obtain the experimental data in the previous research works, and MAPD, indicating the deviation between the predicted results calculated using Eq. (2) and Eq. (10) and the experimental results.

Study	PHE geometrical parameters						Working fluid	T_{sat} (°C)	G (kg/m²s)	Heat transfer process	MAPD (%)	
	β (º)	b (mm)	λ (mm)	D_h (mm)	φ	N^1					Heat transfer	Pressure drop
Yan et al. [14]	60	3.3	10	5.4	1.23	3	R134a	27, 31 and 36	60	Partial condensation: x_m = 0.11 to 0.88	23.1	20.2
Kuo et al. [8]	60	3.3	10	5.4	1.23	3	R410a	20	50, 100 and 150	Partial condensation: x_m = 0.10 to 0.85	15.2	9.2
Longo [25]	65	2	8	3.5	1.14	10	Propylene	25 and 40	7 to 28	Complete condensation: x_{in} = 0.95 to 1 and x_{out} = 0 to 0.01	11.0	19.8
Longo and Zilio [26]	65	2	8	3.5	1.14	10	R1234yf	40	12 to 40	Complete condensation: x_{in} = 0.95 to 1 and x_{out} = 0 to 0.09	12.2	24.8
This study	65	2	7	3.4	1.18	16	R236fa, R245fa, R1233zd(E), Isobutane, R134a, R1234ze(E) and Propane	30, 40, 50, 70, 80 and 90	12 to 93	Complete condensation: ΔT_{sup} = 0 to 5 K and x_{out} = 0.01 to 0.05	8.9	10.3

[1] N: number of plates in the tested PHE

In order to further evaluate the applicability of the heat transfer and pressure drop correlations (Eq. (2) and Eq. (10)) developed in the paper, we used the correlations to predict four sets of experimental data collected from the previous research works. Table 4 summarizes the working conditions and PHE geometrical parameters of the four research works as well as the prediction results in terms of the MAPD. The first two sets of data collected from Kuo et al. [8] and Yan et al. [14] were obtained for partial condensation with the mean vapour quality of the condensation process varying from 0.10 to 0.88. The other two sets of data reported by Longo [25] and Longo and Zilio [26] were obtained for complete condensation, agreeing with our study, but using two working fluids not considered in our work, propylene and R1234yf. As shown in Table 4, the heat transfer correlation has MAPDs of 23.1 %, 15.2 %, 11.0 % and 12.2 % for the four sets of experimental data, respectively, while the pressure drop correlation has MAPDs of 20.2 %, 9.2 %, 19.8 % and 24.8 %, respectively. Figure 9 presents the predicted values calculated using Eq. (2) and Eq. (10) against the experimental data of previous works.

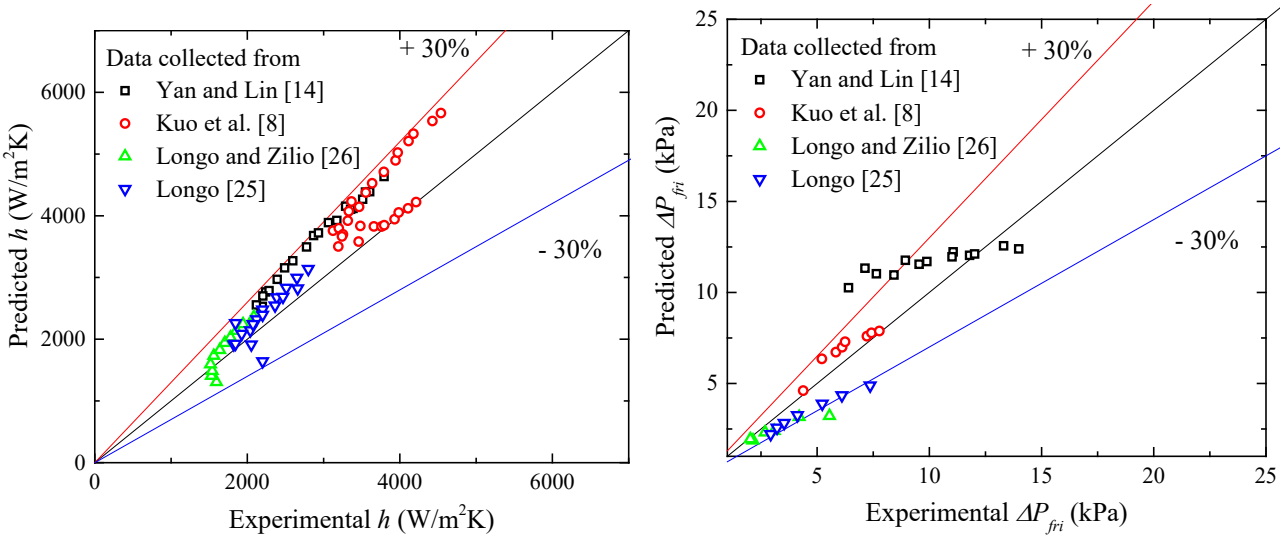

Figure 9 Comparison between the predicted values using Eq. (2) and Eq. (10) and the experimental data collected from the previous research works [8,14,25,26].

4. Discussion

Although the correlations derived by Longo et al. [7] and Kuo et al. [8] have the best predictive performance for the database of 2376 heat transfer data points compiled by Tao and Ferreira [6], they fail to provide the best prediction for a much smaller database (283 data points) obtained in this study among selected existing correlations. This may be because each correlation targets different heat transfer processes. In the correlation derived by Longo et al. [7], the condensation heat transfer is considered to be in the gravity-controlled region as $Re_{eq} < 1600$, and the heat transfer of laminar film condensation in the region is calculated using the Nusselt equation. However, all the test data in this study, also including data points with $Re_{eq} < 1600$, belong to the shear-controlled region, demonstrated by a strong dependence of the heat transfer performance on the flow rate of the working fluids. The correlation from Kuo et al. [8] was developed from the partial condensation in which the x_m of the condenser is used as an important variable, ranging from about 0.1 to 0.9. This is different from a close to complete condensation applied in this study in which the mean vapour quality is always about 0.5. In addition, the discrepancy in evaluation results may be due to the differences in terms of mass fluxes and saturation temperatures in the databases. The database in this study includes data for a wider range of mass fluxes and higher saturation temperatures than the database compiled by Tao and Ferreira [6]. The contradiction in evaluation results indicates that a careful selection of the correlation based on the specific application is needed.

The effects of the condensation temperature on the heat transfer process mainly result from the variation of the thermo-physical properties of the working fluids (e.g. the vapour density, density ratio of liquid to vapour phase and surface tension). The variation of temperature does not change the heat transfer mechanism, i.e. the convective condensation dominates the heat transfer process for the whole range of condensation temperatures in this study. Moreover, when using existing correlations that were developed using the data with relatively low condensation temperatures to predict the experimental results of a given working fluid, the prediction

accuracy is almost independent of the condensation temperature. This observation indicates that for the conditions of shear-controlled condensation, correlations can be applicable for temperatures that are out of the range of temperatures used for the correlation development. However, a wider range of temperature data will contribute to an increased reliability of extending the temperature applicability of the correlation.

The MAPD results presented in Table 4 indicate that the correlations developed in this study are able to predict the results of other works with a deviation of less than 30 % (except for a few data points for the pressure drop correlation), which is in agreement with engineering standard [5]. Specifically, the correlations are able to predict the results of other working fluids (propylene and R1234yf) than those used to derive the correlation. This may be attributed to the fact that working fluids covering a wide range of thermo-physical properties were used to derive the correlation. Furthermore, though the correlations were derived for experimental results of complete condensation, the comparison with previous works suggests that the correlations are able also to predict also the experimental results of partial condensation, covering only a narrow range of vapour quality between the condenser inlet and outlet.

Only one PHE was tested in the study, and thus the correlations were developed without considering the effects of PHE geometry on the thermal-hydraulic performance. A review work [27] found that the shear-controlled condensation is able to be enhanced by increasing the chevron angle of the corrugation. This is attributed to more turbulence in the flow caused by the larger chevron angle. The PHE used in the study has a relatively large chevron angle, 65 °, with respect to the range of chevron angles used in previous research works (27 ° to 70 ° [27]), indicating that the heat transfer performances presented in the current paper are relatively high. In addition, the results of the limited comparison with previous works (see Table 4) suggests that the correlations are applicable also to other heat exchanger geometries. As shown in Table 4, the PHE geometrical parameters considered in Refs. [25,26] are almost identical to those of the PHE considered in our analysis, while the PHE used in Refs. [8,14] has larger dimensions than the PHE considered in our work. However, all the three PHEs can be categorized as small-scale heat exchangers. An evaluation of the applicability of the correlations for PHEs covering a wider range of geometrical parameters (e.g. large-scale channels and smaller chevron angles) remains to be done.

5. Conclusion

A comprehensive experimental investigation using seven organic fluids as working fluids and covering a wide range of condensation temperatures was conducted for developing the prediction methods of flow condensation in plate heat exchangers tailored specifically for organic Rankine cycle and heat pump systems. Four existing heat transfer correlations and two existing pressure drop correlations were used for predicting the experimental results obtained. New correlations were developed, considering two dimensionless numbers, the density ratio and the Bond number, accounting for the shear stress of the vapour phase on the liquid phase, the transition from macroscale to microscale two-phase flow and the surface tension effect.

The results suggest that the frictional pressure drop and heat transfer coefficient both increase with the increase of mass fluxes and decrease with the increase of condensation temperatures, indicating that shear-controlled condensation is dominating in the whole range of working conditions. Due to the lower vapour density and higher surface tension, and hence the more intensified convection at the liquid-vapour interface, R1233zd(E), isobutane and R245fa have a higher heat transfer coefficient than the other working fluids. Moreover, R1233zd(E), R236fa and R245fa have a higher frictional pressure drop due to their larger density ratio of liquid phase to vapour phase. The correlations derived by Yan et al. [14] and Zhang et al. [13] provided the best prediction for the heat transfer coefficient and frictional pressure drop with a mean absolute percentage deviation of 15.2 % and 23.5 %, respectively. Moreover, the results suggest that improved prediction accuracies are achieved with the new correlations, giving a mean absolute percentage deviation of 8.9 % and 10.3 % for the heat transfer coefficient and the frictional pressure drop, respectively. A comparison with results of previous works indicates that the developed correlations are able to predict with reasonable accuracy the results of previous works considering other work fluids, heat exchanger geometries and operating conditions than those used to derive the correlations. Finally, it needs to be stressed that the correlations developed in the paper were obtain for a single plate heat exchanger geometry. The results of the limited comparison of the correlations with previous works suggests that the correlations are applicable also to other heat exchanger geometries, however, a thorough evaluation of the heat transfer and pressure drop correlations' applicability to plate heat exchangers covering a broad range of geometrical parameters remains to be done.

Acknowledgements

The research presented in the paper has received funding from Innovation Fund Denmark with the THERMCYC project (www.thermcyc.mek.dtu.dk, project ID: 1305-00036B), and COWIfonden (Reference A-139.16) was used for the oil heating system building. The financial support is gratefully acknowledged.

References

[1] S. Jin, P. Hrnjak, A new method to simultaneously measure local heat transfer and visualize flow boiling in plate heat exchanger, Int. J. Heat Mass Transf. 113 (2017) 635–646. https://doi.org/10.1016/j.ijheatmasstransfer.2017.04.116.

[2] S. Quoilin, M. Van Den Broek, S. Declaye, P. Dewallef, V. Lemort, Techno-economic survey of organic rankine cycle (ORC) systems, Renew. Sustain. Energy Rev. 22 (2013) 168–186. https://doi.org/10.1016/j.rser.2013.01.028.

[3] H. Lee, Y. Hwang, R. Radermacher, H.H. Chun, Thermal and hydraulic performance of sinusoidal corrugated plate heat exchanger for low temperature lift heat pump, Int. J. Refrig. 36 (2013) 689–700. https://doi.org/10.1016/j.ijrefrig.2012.11.008.

[4] J. Lee, K.S. Lee, Friction and Colburn factor correlations and shape optimization of chevron-type plate heat exchangers, Appl. Therm. Eng. 89 (2015) 62–69. https://doi.org/10.1016/j.applthermaleng.2015.05.080.

[5] F. Vakili-farahani, R.L. Amalfi, J.R. Thome, Two-phase Heat Transfer and Pressure Drop within Plate Heat Exchangers, in: Encycl. Two-Phase Heat Transf. Flow II, 2015: pp. 145–215.

[6] X. Tao, C.A.I. Ferreira, Heat transfer and frictional pressure drop during condensation in plate heat exchangers : Assessment of correlations and a new method, Int. J. Heat Mass Transf. 135 (2019) 996–1012. https://doi.org/10.1016/j.ijheatmasstransfer.2019.01.132.

[7] G.A. Longo, G. Righetti, C. Zilio, A new computational procedure for refrigerant condensation inside herringbone-type Brazed Plate Heat Exchangers, Int. J. Heat Mass Transf. 82 (2015) 530–536. https://doi.org/10.1016/j.ijheatmasstransfer.2014.11.032.

[8] W.S. Kuo, Y.M. Lie, Y.Y. Hsieh, T.F. Lin, Condensation heat transfer and pressure drop of refrigerant R-410A flow in a vertical plate heat exchanger, Int. J. Heat Mass Transf. 48 (2005) 5205–5220. https://doi.org/10.1016/j.ijheatmasstransfer.2005.07.023.

[9] R.L. Amalfi, F. Vakili-Farahani, J.R. Thome, Flow boiling and frictional pressure gradients in plate heat exchangers. Part 2: Comparison of literature methods to database and new prediction methods, Int. J. Refrig. 61 (2016) 185–203. https://doi.org/10.1016/j.ijrefrig.2015.07.009.

[10] H.J. Kim, L. Liebenberg, A.M. Jacobi, Flow visualization of two-phase R-245fa at low mass flux in a plate heat exchanger near the micro-macroscale transition, Sci. Technol. Built Environ. 0 (2019) 1–12. https://doi.org/10.1080/23744731.2019.1648980.

[11] J.R. Thome, Mini- and Microchannel Condensation, in: Encycl. Two-Phase Heat Transf. Flow I, 2015: pp. 231–284. https://doi.org/10.1142/9789814623216_0015.

[12] H.S. Wang, J.W. Rose, A theory of film condensation in horizontal noncircular section microchannels, J. Heat Transfer. 127 (2005) 1096–1105. https://doi.org/10.1115/1.2033905.

[13] J. Zhang, M.R. Kærn, T. Ommen, B. Elmegaard, F. Haglind, Condensation heat transfer and pressure drop characteristics of R134a, R1234ze(E), R245fa and R1233zd(E) in a plate heat exchanger, Int. J. Heat Mass Transf. 128 (2019) 136–149. https://doi.org/10.1016/j.ijheatmasstransfer.2018.08.124.

[14] Y.-Y. Yan, H.-C. Lio, T.-F. Lin, Condensation heat transfer and pressure drop of refrigerant R-134a in a plate heat exchanger, Int. J. Heat Mass Transf. 42 (1999) 993–1006. https://doi.org/10.1016/S0017-9310(98)00217-8.

[15] A. David, B.V. Mathiesen, H. Averfalk, S. Werner, H. Lund, Heat Roadmap Europe: Large-scale electric heat pumps in district heating systems, Energies. 10 (2017) 1–18. https://doi.org/10.3390/en10040578.

[16] C. Wieland, D. Meinel, S. Eyerer, H. Spliethoff, Innovative CHP concept for ORC and its benefit compared to conventional concepts, Appl. Energy. 183 (2016) 478–490. https://doi.org/10.1016/j.apenergy.2016.08.193.

[17] J. Bao, L. Zhao, A review of working fluid and expander selections for organic Rankine cycle, Renew. Sustain. Energy Rev. 24 (2013) 325–342. https://doi.org/10.1016/j.rser.2013.03.040.

[18] B. Zühlsdorf, J.K. Jensen, B. Elmegaard, Heat pump working fluid selection — economic and thermodynamic comparison of criteria and boundary conditions Choix du fluide actif de la pompe à chaleur : comparaison économique et thermodynamique des critères et des conditions limites, 98 (2019) 500–513. https://doi.org/10.1016/j.ijrefrig.2018.11.034.

[19] E.W. Lemmon, I.H. Bell, M.L. Huber, M.O. McLinden, NIST Standard Reference Database 23: Reference Fluid Thermodynamic and Transport Properties-REFPROP, Version 10.0, National Institute of Standards and Technology, Standard Reference Data Program: Gaithersburg, 2018., in: n.d.

[20] S.J. Kline, F.A. McClintock, Describing uncertainties in single-sample experiments, Mech. Eng. 75 (1953) 3–8.

[21] G.A. Longo, Refrigerant R134a condensation heat transfer and pressure drop inside a small brazed plate heat exchanger, Int. J. Refrig. 31 (2008) 780–789. https://doi.org/10.1016/j.ijrefrig.2007.11.017.

[22] F. Vakili-Farahani, R.L. Amalfi, J.R. Thome, Two-Phase Flow and Boiling of R245Fa in a 1 Mm Pressing Depth Plate Heat Exchanger - Part I: Adiabatic Pressure Drop, Interfacial Phenom. Heat Transf. 2 (2014) 325–342. https://doi.org/10.1615/interfacphenomheattransfer.2015012027.

[23] D.H. Han, K.J. Lee, Y.H. Kim, The characteristics of condensation brazed plate heat exchangers with different chevron angles, J. Korean Phys. Soc. 43 (2003) 66–73. https://doi.org/10.1016/S1359-4311(03)00061-9.
[24] Y.Y. Hsieh, T.F. Lin, Evaporation Heat Transfer and Pressure Drop of Refrigerant R-410A Flow in a Vertical Plate Heat Exchanger, J. Heat Transfer. 125 (2003) 852. https://doi.org/10.1115/1.1518498.
[25] G.A. Longo, Heat transfer and pressure drop during hydrocarbon refrigerant condensation inside a brazed plate heat exchanger, Int. J. Refrig. 33 (2010) 944–953. https://doi.org/10.1016/j.expthermflusci.2011.01.018.
[26] G.A. Longo, C. Zilio, Condensation of the lowGWPrefrigerant HFC1234yf inside a brazed plate heat exchanger, Int. J. Refrig. 36 (2013) 612–621. https://doi.org/10.1016/j.ijrefrig.2013.08.013.
[27] J. Zhang, X. Zhu, M.E. Mondejar, F. Haglind, A review of heat transfer enhancement techniques in plate heat exchangers, Renew. Sustain. Energy Rev. 101 (2019) 305–328. https://doi.org/10.1016/j.rser.2018.11.017.